



Strathprints Institutional Repository

Rosochowska, M. and Rosochowski, A. and Olejnik, L. (2009) *Finite element analysis of forward extrusion of 1010 steel*. Annals of Dunărea de Jos, University of Galați, Fascicle V, Technologies in Machine Building. ISSN 1221-4566

Strathprints is designed to allow users to access the research output of the University of Strathclyde. Copyright © and Moral Rights for the papers on this site are retained by the individual authors and/or other copyright owners. You may not engage in further distribution of the material for any profitmaking activities or any commercial gain. You may freely distribute both the url (<http://strathprints.strath.ac.uk/>) and the content of this paper for research or study, educational, or not-for-profit purposes without prior permission or charge.

Any correspondence concerning this service should be sent to Strathprints administrator: <mailto:strathprints@strath.ac.uk>

FINITE ELEMENT ANALYSIS OF COLD FORWARD EXTRUSION OF 1010 STEEL

Malgorzata Rosochowska¹, Andrzej Rosochowski¹, Lech Olejnik²

¹Desing, Manufacture and Engineering Management, University of Strathclyde – 75 Montrose Street, Glasgow G1 1XJ, United Kingdom,

²Institute of Manufacturing Techniques, Warsaw University of Technology – Narbutta 85, 02-524 Warsaw, Poland

E-mail: m.rosochowska@strath.ac.uk

ABSTRACT

Reliability of FE simulation of metal forming processes depends critically on the proper definition of material properties, the friction boundary conditions and details of the FE approach. To address these issues, the room temperature strain hardening behaviour of 1010 steel was established by performing a uniaxial compression test for the true strain of up to 1.5. Friction was evaluated using a ring test, with the two faces of the ring coated with a phosphate conversion layer and soap; the friction experimental results were matched with the FE established reference curves. The experimentally obtained material and friction input data were used in FE simulation, employing Arbitrary Lagrangian Eulerian adaptive meshing, to provide a valuable insight into the process of forward extrusion of an industrial component.

KEYWORDS: FE modelling, friction, extrusion, work hardening

1. INTRODUCTION

The work presented in this paper was performed within a benchmark of finite element (FE) simulation of an industrial cold forward extrusion process of AISI 1010 steel that was carried out under the EU Coordination Action on Virtual Intelligent Forging (VIF). The extruded part was a small axisymmetric automotive component extruded from a cylindrical billet with a diameter of 7.15 mm and a length of 28 mm. The billet was cropped from a drawn bar and coated with a layer of phosphate and soap. The punch stroke during extrusion was 5 mm while the diameter of the extruded end was reduced by 38.7%. The shape of the die used in this process is shown in fig 1. The benchmark dealt with issues such as characterisation of material properties, identifying boundary conditions and the use of different FE codes. Some of the results obtained by the VIF partners were reported at the 12th International Conference on Metal Forming in 2008 [1-3]. Characterisation of friction conditions in cold forging was addressed in [1], where the friction factor was derived using four different tests. The FE simulations of the extrusion process, using a commercial code Abaqus Standard (implicit solver) and Forge 2007, were discussed in detail in [2] and [3]. In the former,

the Coulomb friction coefficient of 0.1 was assumed while in the latter a friction factor of 0.07, derived in the double cup extrusion test, was used. Since the number of partner contributions was limited and the techniques tested not fully explored, the aim of this paper is to extend the pool of results of this benchmark.

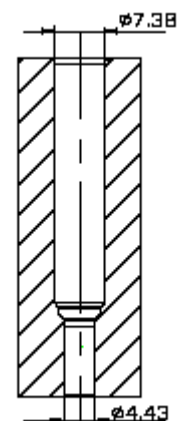


Fig.1. Die insert used for forward extrusion

In any FE simulation of metal forming, reliable results can only be obtained when the material input data and the friction boundary conditions are well

defined. Therefore much attention was paid to these aspects of the process before the FE simulation using Abaqus Explicit was initiated.

2. MATERIAL PROPERTIES

Strain hardening of the investigated steel was tested at room temperature using a laboratory 250 kN press equipped with a hydraulic servo-actuator with a load cell (fig. 2). A dedicated compression rig, with guided platens and the attached displacement transducer (LVDT), was installed on this press (fig. 2).

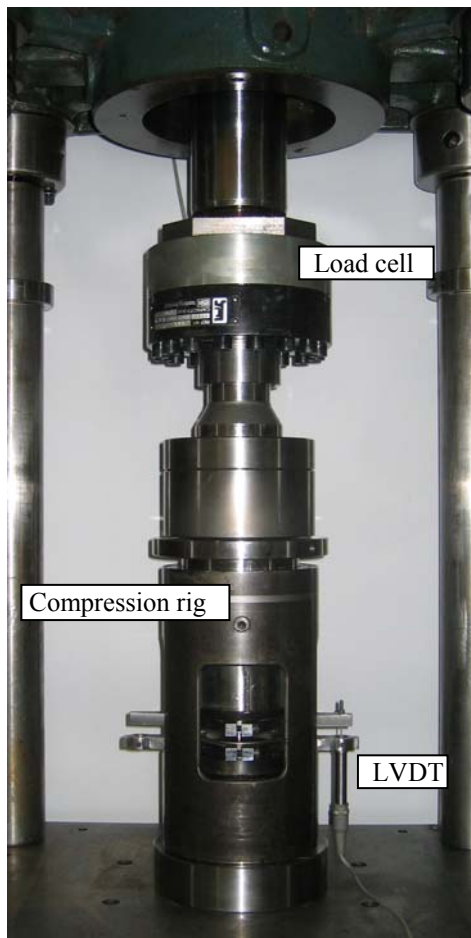


Fig.2. Compression rig

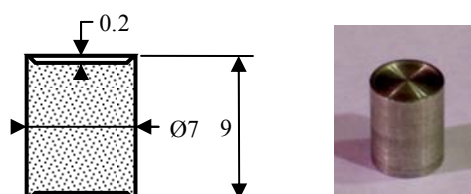


Fig.3. Compression specimen

Cylindrical specimens Ø7x9 (fig. 3), with a small recess on both ends (Rastegaev type) for placing a lubricant, were compressed between the platens at the constant force rate of approximately 2.7

kN/s. The average strain rate in this mode was 3.36×10^{-2} 1/s; increasing the strain rate by the order of one did not affect the response of the material.

Fig. 4 displays the force-height results obtained in the test. The lack of ideally smooth curve resulted from the servo valve misbehaving (this indicates that sudden changes of the force rate have a slight influence on the force level after all). Initially, the force-height curve had a small elastic stiffness of 80 kN/mm, which at the end of the test rose to 705 kN/mm. Assuming that stiffness changes linearly with time between these two values, a strain hardening curve has been obtained as illustrated in fig. 5. The equation approximating the experimental strain hardening curve has been found to be:

$$\sigma = 680(0.1 + \varepsilon)^{0.29} \quad (1)$$

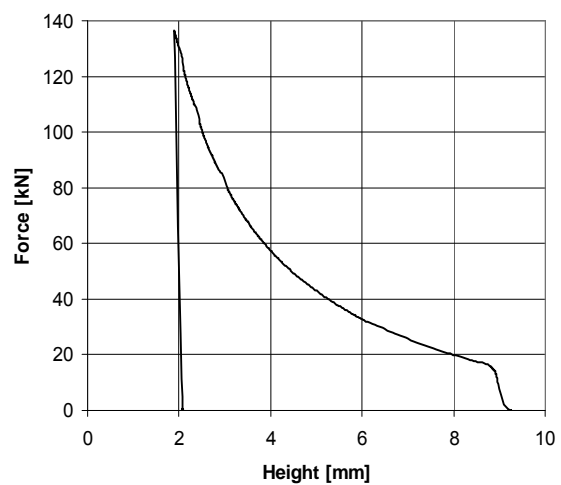


Fig.4. Force-height curve obtained in uniaxial compression test

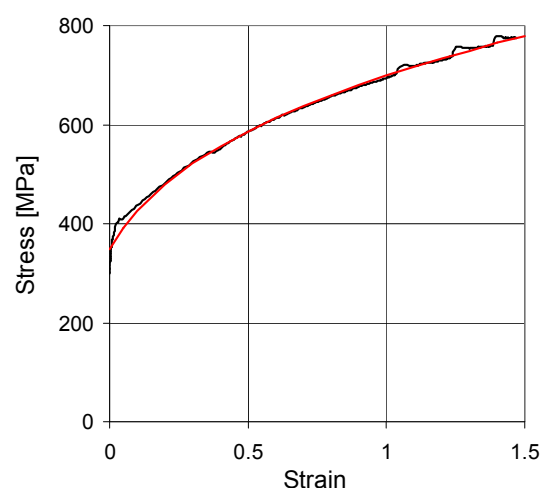


Fig.5. Strain hardening curve

The elastic properties of the investigated steel, that is Young's modulus and Poisson's ratio, were assumed to be $E=210$ GPa and $\nu=0.3$ respectively.

3. FRICTION TEST

Friction was evaluated using the ring test. Specimens, with the outer diameter of 7 mm and the dimensional ratios of 6:3:2 (outer dia.: internal dia.: height), were used in experiments. All specimens were ground to $Ra=0.5 \mu\text{m}$ and coated with a layer of phosphate and soap to replicate surface conditions of the billet used in the forward extrusion process. The geometrical changes of the rings were mapped on the FE established reference curves to find a Coulomb friction coefficient. The reference curves were computed using strain hardening properties described in the previous section by equation (1). The tests were carried out at a strain rate of $3.36 \times 10^{-2} \text{ 1/s}$ that is the same at which strain hardening properties were derived. The reduction of the specimen's height ranged from 15% to 55%; results are shown in fig. 6.

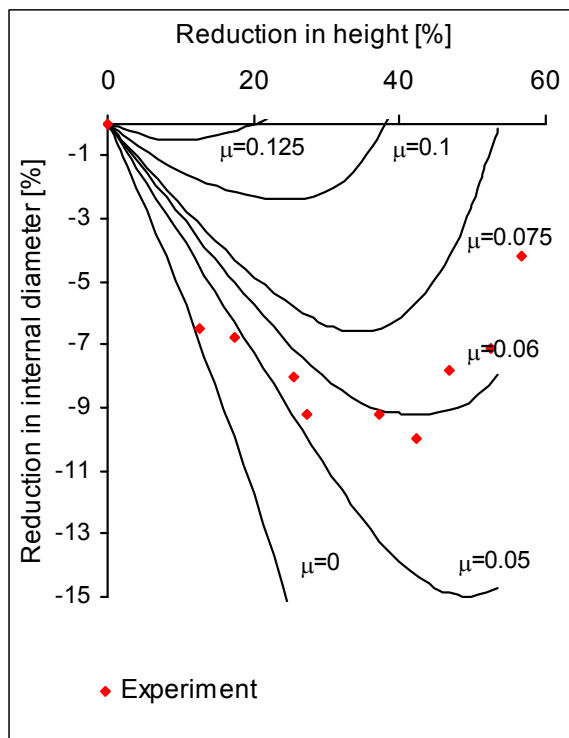


Fig.6. Reference curves and experimental points used to derive friction coefficient

Friction conditions changed with deformation. For the height reduction of up to 30%, the friction coefficient was about 0.05, while for the height reduction of 55% it reached nearly 0.7. Therefore the average friction coefficient for the investigated range was assumed to be 0.06; similar magnitude of the friction coefficient was obtained in the test, which was the replica of the investigated forward extrusion process carried out in a controlled laboratory environment [1].

4. FE MODEL

The simulation was carried out using the Abaqus Explicit code. A 2D axisymmetric model was used. The die and punch were modelled as rigid bodies. The axisymmetric 4-node elements, CAX4, were used to mesh the billet. To accommodate the smallest feature of the die geometry, which had a radius of 0.3 mm, and prevent penetration of the billet into the die, the billet was meshed using a graded mesh with the 0.05mm long elements in the close vicinity of the die surface. The high distortion of the finite elements due to nearly 40% reduction of the billet diameter, and additional shear near the die surface, required re-meshing of the billet. In Abaqus Explicit, distortion of the mesh may be controlled using an Arbitrary Lagrangian Eulerian (ALE) adaptive technique for meshing; the topology of the mesh remains unchanged during the analysis and the mesh is adapted by smoothing off the node positions. Only mesh of the extruded section of the billet was subjected to adaptive meshing. The initial mesh and the mesh used in the last simulation increment are shown in fig. 7a and 7b respectively.

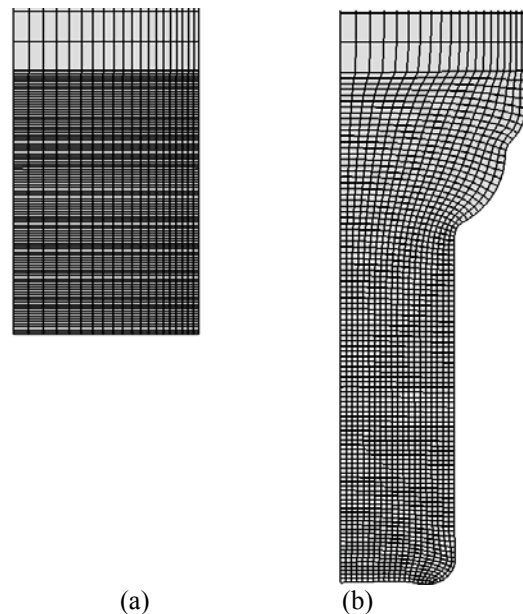


Fig.7. Initial (a) and final (b) mesh resulting from using ALE adaptive meshing technique in Abaqus Explicit

The classical, elastic-plastic, von Mises, strain-hardening, isotropic model of the material was employed as defined in paragraph 2. Friction was modelled using the Coulomb's friction coefficient of $\mu=0.06$ at the die-billet interface and $\mu=0.1$ at the punch face. The material flow and the final product geometry, the strain and stress distributions, the process force and the tool contact pressure have all been obtained providing a valuable insight into the process.

5. FE SIMULATION RESULTS

The flow of the material is illustrated by the equivalent plastic strain contours shown in fig. 8 for four stages of the extrusion process. The maximum calculated strain is 2.46, which is almost two times smaller than that computed using Abaqus Standard [2].

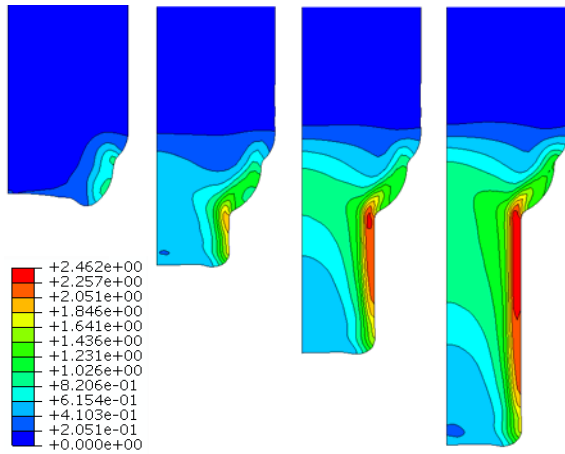


Fig.8. Equivalent plastic strain for punch stroke of 2, 3, 4 and 5 mm

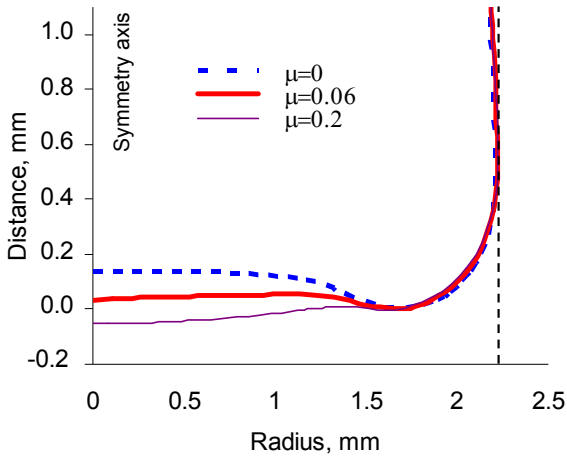


Fig.9. Computed contour of the free end of the extruded component

The industrial component produced by forward extrusion had a 0.6 mm deep recess at the free end of the extruded stem. This feature has been used in [3] to compare the Forge 2007 simulation results for different computational models with the results obtained experimentally; only a 3D simulation, taking into account strain accumulated in the preceding cutting operation of the billet, managed to recreate the recess depth properly (0.5 mm). A 2D simulation, similar to the one reported here, produced a recess 0.18 mm deep. Contrary to these results, the shape of the free end computed using Abaqus Standard was slightly convex [2]. The shape of the extruded component obtained in our work is shown in fig. 7b.

It features a shallow recess at the free end, the details of which are shown in fig. 9. The shape and the maximum depth of this recess depend on the friction coefficient used in the simulation. For $\mu=0.06$, the recess depth is approximately 0.06 mm while for $\mu=0$ it reaches 0.13 mm. For $\mu=0.2$, the free end surface is mainly convex. Further, an increase in the diameter close to the free end was observed (fig. 9). This resulted in a spike in the die contact pressure close to the free end of the stem during the whole process; this is clearly visible in fig 10, which illustrates the die contact pressure distribution for the last stage of the process.

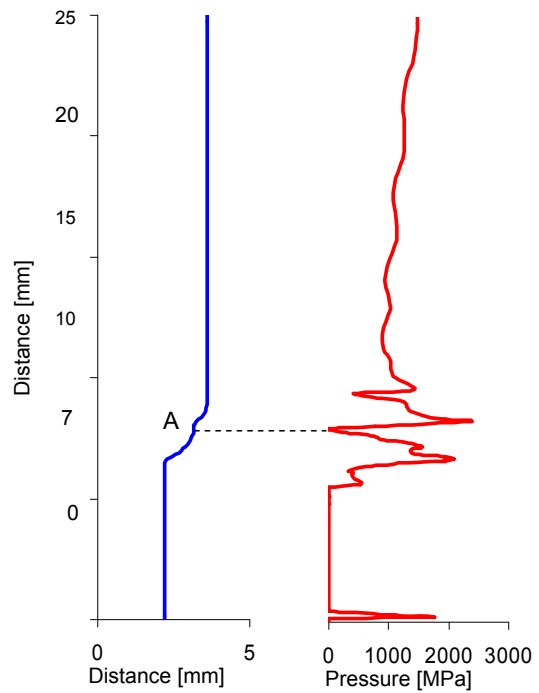


Fig.10. Contact pressure distribution along the die surface

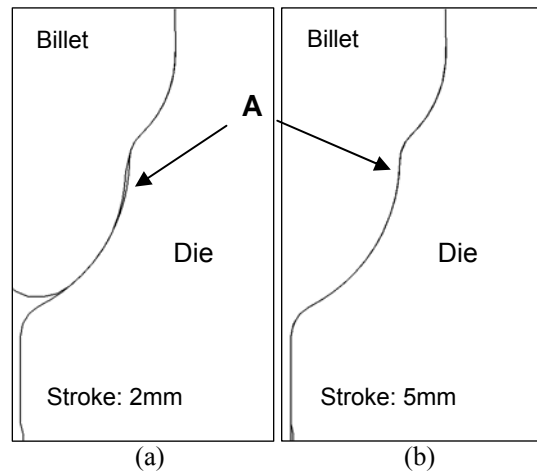


Fig.11. Gap between billet and die for punch stroke of 2 mm (a) and 5 mm (b)

Another interesting feature in fig. 10 is the contact pressure drop in the middle of the die deformation zone, in the area marked A. It is due to a gap created at the early stage of the process (fig. 11a); this gap gradually diminishes and is hardly visible at the end of the process (fig 11b), however, it never completely disappears. A smaller pressure drop is observed at the entrance to the die deformation zone, which, similarly to the pressure drop described earlier, is caused by the material having problems with following the high curvature die contour.

The history of the forming force versus punch stroke for different friction conditions is shown in fig.12. The dramatic differences in the maximal force confirm the major effect of friction in forward extrusion. There are three stages of the process, which are clearly visible. The initial reduction of the billet diameter is accompanied by a gradual force increase, further reduction leads to a steep rise of the force, followed by stabilisation of the force towards the end of the process. However, there is no force reduction often observed in the last stage of forward extrusion due to reduced friction in the container part of the die. The constant value of the force obtained for the case without friction confirms the stationary character of the process and validates the FE model.

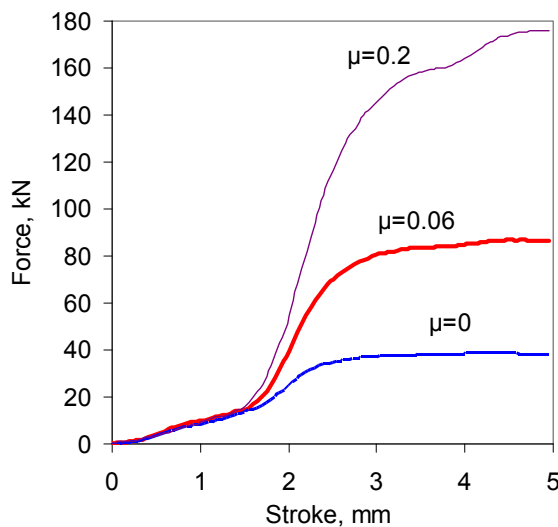


Fig.12. Forming force versus punch stroke for different friction conditions

6. DISCUSSION

It is universally recognised that reliable input data, together with sound computational FE algorithm, are required to obtain valid simulation results for metal forming processes. However, very often, some of these requirements are not met, which leads to wrong simulation results and consequently wrong conclusions. In this paper, an effort has been made to address the three critical aspects of process simulation that is obtaining reliable data on strain hardening of the processed material, establishing friction behaviour for a given coating/lubricant

applied and using a robust FE algorithm to deal with large distortion of FE elements and changing contact conditions.

Regarding strain hardening characterisation, it is logical that for bulk metal forming operations, featuring large strains and compressive stresses, a uniaxial compression test is most appropriate [4]. In this context, it is important that the material flow and friction in this test are decoupled. This can be achieved by using the compression specimens with a recess on both ends (Rastegaev type), which acts as a reservoir for lubricant during the test. Normally, the compression test is carried out for the maximum true strain of approximately 1. In our tests, we have reached the strain of 1.5, which was possible because of very good lubrication and lack of barrelling of the cylindrical sample. However, it might be difficult or impossible to increase this strain further, as required in some bulk metal forming operations. In the case of the extruded component analysed here, the maximum equivalent (true) strain was nearly 2.5. This required the extrapolation of the strain hardening curve beyond the measured maximum strain of 1.5 using Eq. 1.

Referring to the compression testing technique, it is advisable to take into account the changing stiffness of the sample during the test as it defines the plastic-elastic split of the strain. Thus it is important that the change of sample height is measured ‘‘close’’ to the sample to avoid the influence of elastic deflection of the test rig and the press/testing machine.

Establishing friction conditions is crucial in bulk metal forming because of the usually high contact pressure and the influence of friction on the material flow, tool stresses and the forming force. Among the many friction tests, the ring compression test combined with FE calibration is most popular [5]. However, as fig. 6 indicates, it is not easy to obtain an unambiguous result in terms of a constant friction coefficient.

Perhaps a better match between the experimental points and the calibration curves could have been obtained for friction factor rather than friction coefficient. On the other hand friction factor is known to be better suited to describe friction in hot forming operations, which was not the case in the process analysed in this paper. It was also another difficulty in applying the friction factor in the Abaqus analysis. Since friction stress calculation is based on the friction factor scaling the current yield stress, it would be beneficial if the evolution of yield stress was taken into account. However, in Abaqus, one can only define a constant value of the shear friction stress (through capping Coulomb friction), unless a user-defined friction subroutine is developed.

There is an ongoing discussion on the appropriate description of friction in bulk metal forming. It is possible that, as suggested in numerous publications of Wanheim and Bay, e.g. [6], a compromise between the Coulomb friction law and

the friction factor approach is the best solution. Nevertheless, it seems that for high pressure in particular, more experimental and fundamental work on friction is still necessary.

Abaqus Explicit is well suited to deal with large deformation and changing boundary conditions. However, highly concentrated deformation may lead to excessive distortion of FE elements and material penetration into the die. A simple method of dealing with this problem is to predict the element distortion and define it "pre-distorted" in the opposite direction, so it becomes more regular when strained. However, it is difficult to do it precisely for different regions of the initial mesh. Therefore various automatic meshing/remeshing schemes are being used. Unfortunately, in Abaqus Explicit, only a limited meshing/remeshing scheme (ALE adaptive meshing) is available which retains the mesh topology. This means that sensible initial meshing is still required. When a new mesh is generated dynamically during the computation process, all field quantities have to be translated from the old mesh to the new one. This may lead to the accumulation of errors. As usual, it is important that common sense and the engineering knowledge of the simulated process are used to critically assess such results.

The FE simulation results presented in this paper seem to be mechanically sound and provide a lot of information about the process. There are some doubts regarding, for example, the slightly oscillating character of tool contact pressure in the die container or the fact that for predicting dimensional accuracy one should take into account tool deflection. However, even with these deficiencies, some interesting observations regarding product properties or process design can be made.

It is clear from fig. 8 that plastic strain distribution is highly non-uniform, which will lead to non-uniform hardness distribution in the cross-section of the extruded component. While the radial inhomogeneity can be beneficial because of the higher hardness of the component surface, the longitudinal one is not good. It results in much softer end of the extruded component, which, together with geometrical requirements, may require cutting it off.

The presence of the contact pressure drops in fig. 10 and gaps in fig. 11, leads to the conclusion that the geometry of the die is not optimal. Provided that the design of the component head allows minor changes in its geometry, it is advisable that the gap areas are avoided by increasing the radii of the die contour. This should have a beneficial effect on the contact pressure distribution making it more uniform and of lower value. The current maximum value of contact pressure of more than 2000 MPa is demanding for the tool, which probably led to the decision to make it of sintered carbide.

The lower spike in the contact pressure distribution in fig. 10, due to an increased stem diameter near its end, suggests that the assumed die

diameter clearance of 0.05 mm is too small. It could be slightly increased without losing its potentially beneficial role as a guide for the stem during extrusion and ejection.

The maximum level of the extrusion force indicated in fig. 12 is helpful in identifying a press with suitable capacity. However, more important is the tool contact stress, which depends on that force. Since the tool contact pressure for $\mu=0.06$ is already very high, any increase of friction causing force increment is not allowed. The sensitivity of extrusion force to the friction coefficient makes forward extrusion a good candidate for a standard friction test.

The motivation for research presented in this paper was to provide more results for a benchmarking exercise. It is clear, that various FE codes produce different results (e.g. Abaqus Standard vs. Abaqus explicit). Equally, the quality of input data differentiates these results. Standardisation of experimental procedures and FE techniques is unlikely in the near future, therefore, comparison of different approaches in the form of a benchmark test should help identify the most promising solutions.

ACKNOWLEDGEMENTS

The financial support provided by EU FP6, within the Coordination Network on Virtual Intelligent Forging (VIF), is gratefully acknowledged.

REFERENCES

- [1] Qin, Z., Felder, E., Arentoft, M., Paldn, N., Dubar, L., Borsetto, F., Bruschi, S., *Results of Friction Benchmark in Cold Forging Condition*, Proceedings of Metal Forming 2008 Conference, Vol. 2, pag. 781-788;
- [2] Vidal-Salle, E., Boyer, J.-C., Bouttaba, S., *Influence of Inertia Effects on An Energy Driven Thermo-Mechanical Forming Process: Contribution To The VIF Benchmark*, Proceedings of Metal Forming 2008 Conference, Vol. 2, pag. 798-804;
- [3] Borsett, F., Simionato, M., Ghiotti, A., Bruschi, S., *Accurate Modelling of The Forming Process Chain To Predict Forged Component Geometry*, Proceedings of Metal Forming 2008 Conference, Vol. 2, pag. 820-825;
- [4] Rosochowski, A., Olejnik, L., Gagne, J., Ladeveze, N., Rosochowska, M., *Compression behaviour of UFG aluminium*, Proc. of the 9th Int. Conference on Material Forming ESAFORM 2006, Glasgow, United Kingdom, April 26-28, 2006, pag. 543-546
- [5] Balendra, R., Rosochowska, M., Chodnikiewicz, K., Smith, R., *Preliminary assessment of the influence of surface microgeometries on friction*, Advanced Technology of Plasticity, Proceedings of the 8th ICTP Conference, Verona, October 2005;
- [6] Wanheim, T., Bay, N., *A model for friction in metal forming processes*, Ann. CIRP 1978 27(1), pag. 189-194;